Journal of Applied Fluid Mechanics, Vol. 9, No. 1, pp. 119-130, 2016.
Available online at www.jafmonline.net, ISSN 1735-3572, EISSN 1735-3645.
DOI: 10.18869/acadpub.jafm.68.224.23962

Partition Effect on Thermo Magnetic Natural Convection and Entropy Generation in Inclined Porous Cavity

H. Heidary[1], M. J. Kermani[1†] and M. Pirmohammadi[2]

[1]*Department of Mechanical Engineering, Amirkabir University of Technology (Tehran Polytechnic), Tehran, Iran*
[2]*Department of Mechanical Engineering , Pardis Branch, Islamic Azad University, Pardis New City, Tehran,* Iran

†Corresponding Author Email: mkermani@aut.ac.ir

(Received August 2, 2014; accepted November 10, 2014)

ABSTRACT

In this study natural convection heat transfer fluid flow and entropy generation in a porous inclined cavity in the presence of uniform magnetic field is studied numerically. For control of heat transfer and entropy generation, one or two partitions are attached to horizontal walls. The left wall of enclosure is heated with a sinusoidal function and right wall is cooled isothermally. Horizontal walls of the enclosure are adiabatic. The governing equations are numerically solved in the domain by the control volume approach based on the SIMPLE technique. The influence of Hartmann number, inclination angle, partition height, irreversibility distribution ratio, and partition location is investigated on the flow and heat transfer characteristics and the entropy generation. The obtained results indicated that the partition, magnetic field and rotation of enclosure can be used as control elements for heat transfer, fluid flow and entropy generation in porous medium.

Keywords: MHD; Free convection; Partition; Porous media.

1. INTRODUCTION

Flow of an ambient fluid induced solely due to buoyancy occurs in several natural and engineering processes. Natural convection in partitioned rectangular porous cavity with various boundary conditions exists in many engineering application like: high performance insulation for buildings, chemical catalytic reactors, the underground spread of pollutants, solar power collectors, and geothermal energy systems.

Effect of non-uniform sinusoidal heated wall in an open square cavity with viscose fluid is studied numerically by Basak and Roy (2005). Other studies of the natural convection in enclosures with sinusoidal temperature boundary condition are due to Bilgen and Yedder (2007), Storesletten and Pop (1996), Saeid (2005) and Heidary *et al*. (2009). They studied natural convection in porous cavity with sinusoidal bottom wall temperature variation. Basak *et al*. (2006) investigated effects of sinusoidal boundary conditions in cavity filled with porous media without porosity. Control of natural convection can be done with boundary condition or adding divider for disturbing fluid flow. In last decades, most of the studies on partition or divider were taken as non-porous medium filled partitioned rectangular or square enclosures. Also Varol *et al*. (2007) investigated the effects of fin location on the bottom wall of a triangular enclosure filled with porous media. The study of an electrically conducting fluid in engineering applications is of considerable interest, especially in metallurgical and metal working processes or in separation of molten metals from nonmetallic inclusions by the application of a magnetic field.

The phase change problem occurs in casting, welding, melting purification of metals and in the formation of ice layers on the oceans as well as on aircraft surfaces. In that case the fluid experiences a Lorentz force and its effect is to reduce the flow velocities. This in turn affects the rate of heat and mass transfer. The homogeneity and quality of single crystals grown from doped semiconductor melts is of interest to the manufacturers of electronic chips. Hence there has been increased interest in the flows of electrically conducting fluid in cavities subjected to external magnetic field. Natural convection flow in the presence of a magnetic field in enclosure heated from one side and cooled from the other side was considered by Ece and Büyük (2006), Jue (2006) and Pirmohammadi and Ghassemi (2009). Free convection in an open cavity by locating partition is

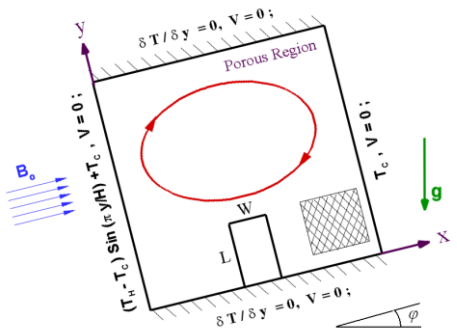

(a)

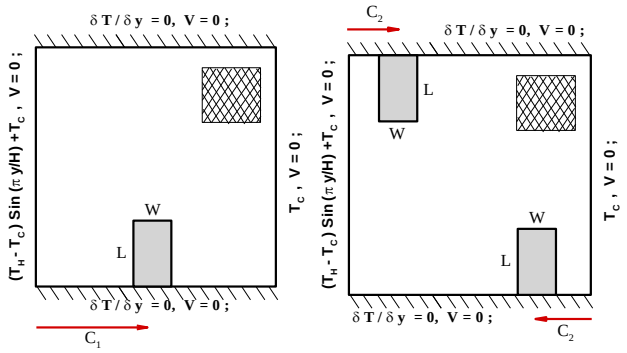

(b)

Fig. 1. (a) - Schematic diagram of the cavity studied in the present computation, (b) - schematic diagram of two types of partition location studied in this paper.

studied by Kandaswamy *et al.* (2008) and Abdul Hakeem *et al*. (2008). Krakov and Nikiforov (2005) and Grosan *et al*. (2009) investigated the effect of magnetic field on free convection heat transfer in porous cavity. Merrikh and Mohamad (2000), Khanafer *et al*. (2000) and Mahmud and Fraser (2004) have simulated magneto hydrodynamics in porous domain at different applications. Fundamentals of entropy generation are presented by Bejan (1994), Rosen (1999) and Narusawa (2001). Magherbi *et al.* (2003) numerically analyzed the entropy generation due to heat transfer and friction in transient state for laminar natural convection. Varol *et al*. (2008) have studied entropy generation due to conjugate natural convection heat transfer and fluid flow inside an enclosure with two solid massive walls in vertical sides at different thicknesses. Mahmud *et al*. (2007) studied flow, thermal, energy transfer, and entropy generation characteristics inside wavy enclosures filled with microstructures. Famouri and Hooman (2008) investigated entropy generation for natural convection by heated partitions in a cavity. Kaluri and Basak (2011 a,b) studied role of entropy generation on thermal management during natural convection in porous and non-porous square cavities with distributed heat sources. Baytas (2000) investigated entropy generation distribution according to inclination angle for saturated porous cavity. The importance of thermal boundary conditions in heat transfer and entropy generation for natural convection inside a porous enclosure investigated by Zahmatkesh (2008).

The effect of magnetic field on entropy generation at the onset of natural convection was studied by Magherbi *et al*. (2010). Mahmud and Fraser (2004) investigated the effect of magnetohydrodynamic free convection and entropy generation in a square porous cavity. To the best of our knowledge no comprehensive model has been published yet to study natural convection on controlling heat transfer and entropy generation by including rectangular partition in porous inclined cavity under magnetic field. In the present study, natural convection in an inclined cavity filled with a porous medium cooled from right wall and heated from the left is analyzed numerically, while flow field is under magnetic field. Also horizontal walls are assumed adiabatic. Because constant thermal boundary condition usually doesn't occur in nature, the hot wall temperature is assumed to be non-uniform temperature distribution prescribed at the left wall. But the difference between uniform and non-uniform boundary conditions has not been studied in this paper. We have studied the effects of non-uniform boundary condition in our earlier paper (2009). The main objective of this study is to control flow pattern, heat transfer and entropy generation in the inclined porous enclosure under magnetic field with one or two partition attached to the horizontal wall. For simulating of porous media, Darcy-Brinckman model is assumed to hold.

2. MATHEMATICAL ANALYSIS

A schematic diagram of a two-dimensional inclined porous cavity under magnetic field is shown in Fig. 1. It is assumed that the right wall of the cavity is cooled to the constant temperature T_C and the left wall is heated to the non-uniform temperature $(T_H - T_C)Sin(\pi y / H) + T_C$, where $T_H > T_C$, and the horizontal walls are adiabatic. The interface between the partition and the porous media is set to adiabatic boundary.

In the porous medium, Darcy-Brinckman model is assumed to hold, and the fluid is assumed to be a normal Boussinesq fluid. With these assumptions, the continuity, momentum and energy equations for steady, two-dimensional flow in an isotropic and homogeneous porous medium under magnetic field are:

$$\frac{\partial u}{\partial x}+\frac{\partial v}{\partial y}=0 \tag{1}$$

$$\frac{1}{\Phi^2}\left(u\frac{\partial u}{\partial x}+v\frac{\partial u}{\partial y}\right)=-\frac{1}{\rho}\frac{\partial p}{\partial x}+\frac{\nu}{\Phi}\left(\frac{\partial^2 u}{\partial x^2}+\frac{\partial^2 u}{\partial y^2}\right) -\frac{\nu}{K}u+g.\sin\phi.\beta\left(T-T_c\right) \tag{2}$$

$$\frac{1}{\Phi^2}\left(u\frac{\partial v}{\partial x}+v\frac{\partial v}{\partial y}\right)=-\frac{1}{\rho}\frac{\partial p}{\partial y}+\frac{\nu}{\Phi}\left(\frac{\partial^2 v}{\partial x^2}+\frac{\partial^2 v}{\partial y^2}\right) -\frac{\nu}{K}v+g.\cos\phi.\beta\left(T-T_c\right)-\frac{\sigma B_0^2}{\rho}\frac{v}{\Phi} \tag{3}$$

$$u\frac{\partial T}{\partial x}+v\frac{\partial T}{\partial y}=\alpha\left(\frac{\partial^2 T}{\partial x^2}+\frac{\partial^2 T}{\partial y^2}\right) \tag{4}$$

where u and v are the seepage velocity components along x- and y- axes, p is pressure, T is the fluid temperature. Also ν, K, φ, Φ and ρ are kinematic viscosity, permeability, inclination angle, porosity and density, respectively. B_0 is the magnitude of magnetic field and σ is the electrical conductivity. The non-dimensional forms of the governing equations (1) – (4) are:

$$\frac{\partial U}{\partial X}+\frac{\partial V}{\partial Y}=0 \tag{5}$$

$$\frac{1}{\Phi^2}(U\frac{\partial U}{\partial X}+V\frac{\partial U}{\partial Y})=-\frac{\partial P}{\partial X}+\frac{\Pr}{\Phi}\left(\frac{\partial^2 U}{\partial X^2}+\frac{\partial^2 U}{\partial Y^2}\right) -\frac{\Pr}{Da}U+Ra\Pr\theta\sin\phi \tag{6}$$

$$\frac{1}{\Phi^2}(U\frac{\partial V}{\partial X}+V\frac{\partial V}{\partial Y})=-\frac{\partial P}{\partial Y}+\frac{\Pr}{\Phi}\left(\frac{\partial^2 V}{\partial X^2}+\frac{\partial^2 V}{\partial Y^2}\right) -\frac{\Pr}{Da}V+Ra\Pr\theta\cos\phi-\frac{1}{\Phi}Ha^2\Pr V \tag{7}$$

$$U\frac{\partial\theta}{\partial X}+V\frac{\partial\theta}{\partial Y}=\left(\frac{\partial^2\theta}{\partial X^2}+\frac{\partial^2\theta}{\partial Y^2}\right) \tag{8}$$

where non-dimensional variables are defined as follows:

$$X=\frac{x}{H}, Y=\frac{y}{H}, U=\frac{uH}{\alpha}, V=\frac{vH}{\alpha}, \theta=\frac{T-T_C}{T_H-T_C},$$
$$P=\frac{pH^2}{\rho\alpha^2}, \Pr=\frac{\nu}{\alpha}, Da=\frac{K}{H^2}, Ra=\frac{g\beta\Delta TH^3}{\nu\alpha}$$
$$\alpha=\frac{\alpha_f}{\lambda}\ , \lambda=k_f/k_e, k_e=\Phi.k_f+(1-\Phi).k_s \tag{9}$$

The effect of the electromagnetic field is introduced into the equations of motion (7) through Hartmann number (Ha). Ha is defined as:

$$Ha=B_0H\sqrt{\frac{\sigma}{\rho\nu}} \tag{10}$$

It is noted that $\frac{1}{\Phi}Ha^2 prV$ in equation (7) is achieved by simplifying the Lorentz force term ($\vec{J}\times\vec{B}$) using constant magnetic field. Boundary conditions as shown in Fig. 1 are:

Left wall $U(0,Y)=0,\ V(0,Y)=0,$

Right wall $U(1,Y)=0, V(1,Y)=0,$

Top wall $U(X,1)=0, V(X,1)=0,$

Bottom wall $U(X,0)=0, V(X,0)=0,$

On the Partition: $U(X,Y)=0, V(X,Y)=0,$

And:

Left wall $\theta(0,Y)=Sin(\pi Y),$

Right wall $\theta(1,Y)=0,$

Top wall $\partial\theta(X,1)/\partial Y=0,$

Bottom wall $\partial\theta(X,0)/\partial Y=0,$

On the Partition: $\partial\theta(X,Y)/\partial n=0;$

The heat transfer coefficient in terms of the local Nusselt number (Nu_y) and average Nusselt number ($\overline{Nu}$) at the left wall are defined by:

$$Nu_y=\left(-\frac{\partial\theta}{\partial X}\right)_{X=0}\ ,\ \overline{Nu}=\int_0^1 Nu_y\,dY \tag{11}$$

Also dimensionless temperature contours (θ) and streamline contours (ψ) are depicted in result section. The stream function ψ is defined as $v=-\partial\psi/\partial x$ and $u=\partial\psi/\partial y$.

The volumetric entropy generation can be obtained from the equation (12):

$$S'''_{gen}=\frac{k_f}{T_0^2}\left(\nabla T\right)^2+\frac{\mu}{KT_0}\left(u^2+v^2\right)+\frac{\sigma B_0^2}{T_0}\frac{v}{\Phi^2}^2 \tag{12}$$

where u and v are seepage velocity (Nield (1999)). The dimensionless form of entropy generation rate S'''_{gen} is termed as entropy generation number. Entropy generation number (OEG) is the ratio between the volumetric entropy generation rate S'''_{gen} and a characteristic transfer rate S'''_0. The characteristic transfer rate for the present problem can be estimated from the following equation:

$$S'''_0=\frac{k_f\left(\Delta T\right)^2}{H^2T_0^2} \tag{13}$$

So the dimensionless overall entropy generation

(OEG) can be expressed as:

$$OEG = \frac{S'''_{gen}}{S'''_0} = \left[\left(\frac{\partial\theta}{\partial X}\right)^2 + \left(\frac{\partial\theta}{\partial Y}\right)^2\right] + \varphi\left[\left(U^2+V^2\right) + \left(Ha*\right)^2\frac{V^2}{\Phi^2}\right] \quad (14)$$

Where

$$\left(Ha*\right)^2 = Da.Ha^2;\quad Ha^* = B_0\sqrt{\frac{\sigma K}{\mu}}\ or\ Ha^* = B_0 H\sqrt{\frac{\sigma Da}{\mu}} \quad (15)$$

where $Ha*$ is Hartmann number in case of porous media.

The non-dimensional volumetric entropy generation due to heat transfer irreversibility (HTI) and fluid frictional irreversibility (FFI) can be obtained by the following equations:

$$HTI = \left(\frac{\partial\theta}{\partial X}\right)^2 + \left(\frac{\partial\theta}{\partial Y}\right)^2 \quad (16)$$

$$FFI = \varphi\left[\left(U^2+V^2\right) + \left(Ha*\right)^2\frac{V^2}{\Phi^2}\right] \quad (17)$$

where θ, U, V, X, Y are the dimensionless temperature, velocity components and Cartesian coordinates respectively and ϕ is irreversibility distribution ratio:

$$\phi = \frac{\mu T_\circ}{k_f}\left(\frac{\alpha^2}{K(\Delta T)^2}\right);\quad T_o = \frac{T_H + T_C}{2} \quad (18)$$

The overall entropy generation (OEG) in the flow field can be obtained by:

$$OEG = HTI + FFI \quad (19)$$

The Bejan number (Be) which describes the contribution of heat transfer entropy on overall entropy generation is defined by:

$$\text{Be} = \frac{HTI}{FFI + HTI} \quad (20)$$

On the other hand, Bejan number (Be) is the ratio of HTI to the total entropy generation (OEG). Bejan number ranges from 0 to 1. Accordingly, Be = 1 is the limit at which the heat transfer irreversibility dominates, Be = 0 is the opposite limit at which the irreversibility is dominated by fluid friction effects, and Be = 0.5 is the case in which the heat transfer and fluid friction entropy generation rates are equal.

3. NUMERICAL PROCEDURES

This code uses Finite Volume method and the SIMPLE algorithm developed by Patankar and Spalding (1972) for discretizing the governing equations of flow and resolving the pressure-velocity coupling system. In addition, all the variables are stored in same nodes by using collocated grid. This method was suggested by Rhie and Chow (1983). Collocated grid has various advantages over the staggered grid, e.g. the control volumes for all variables coincide with the boundaries of the solution domain, facilitating the enforcement of boundary conditions, and giving a simplified data storage structure. The diffusion term of the equations is discretized using a central difference algorithm. As the convergence criterion, 10^{-5} is chosen for all dependent variables, where the computation is terminated if $\sum_{i,j}\left|\Lambda^n_{i,j} - \Lambda^{n-1}_{i,j}\right| \Big/ \sum_{i,j}\left|\Lambda^n_{i,j}\right| \le 10^{-5}$. Here Λ stands for either temperature or velocity components, and n denotes the iteration step.

Table 1 shows the grid-independency test in this study. Four grid sizes (32 × 32, 64 × 64, 100 × 100, and 128 × 128) are chosen for analysis. Average Nusselt number for all four grid sizes are monitored at Ra = 5×10^6, Ha = 50, $\phi = 0^o$ and in case of two partitions. The magnitude of average Nusselt number at 128 × 128 grids shows a very little difference with the result obtained at 100 × 100 grids (0.23%). So we chose a grid size of 100 × 100 for our calculation in this paper.

Table 1 Validations Grid independency test for *Ra* = 5×10⁶, *Ha* = 50, $\varphi = 0^o$ and two partitions

Grid dimension (*X* by *Y*)	Average Nusselt number	Difference with previous coarse mesh (%)
32×32	3.617	--
64×64	3.816	5.50
100×100	3.895	2.07
128×128	3.904	0.23

Table 2 Validations: comparison of average Nusselt number obtained from the present computation and that of the literature for a porous enclosure (cavity) at various Ra, *Da* = 10^{-2} and Φ = 0.9

Re	Present study	Nithiarasu *et al.* (1997)	Deviation % (Abs)
103	1.019	1.02	0.10
104	1.684	1.7	0.95
105	4.117	4.19	1.77
5×105	6.997	7.06	0.90

4. RESULTS AND DISCUSSION

Schematic of the computational domain is shown in Figs. 1-(a) and (b). Fig. 1-(b) shows two types of partition location studied in this paper.

In order to assess the accuracy of our numerical procedure, we have tested our algorithm for the classical natural convection problem in porous and non-porous cavity with adiabatic top and bottom walls and differentially heated side walls. For the

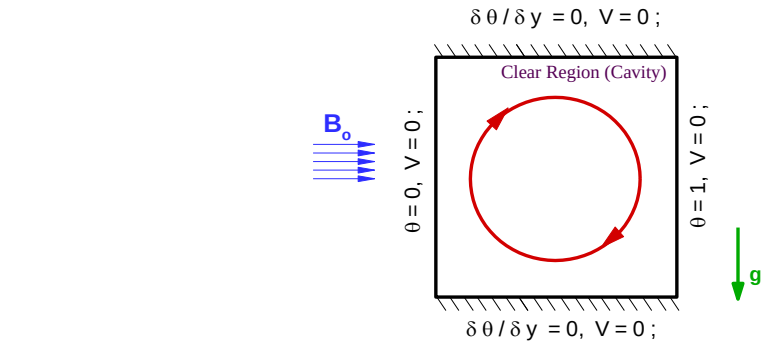

(a)

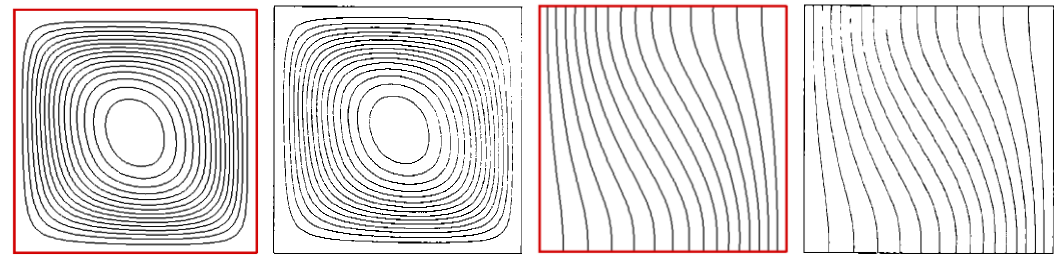

Streamline, Present work | Streamline, Sarris *et al*. (2006) | Isotherm, Present work | Isotherm, Sarris *et al*. (2006)

(b) **Ra = 7×10^3, Ha = 25**

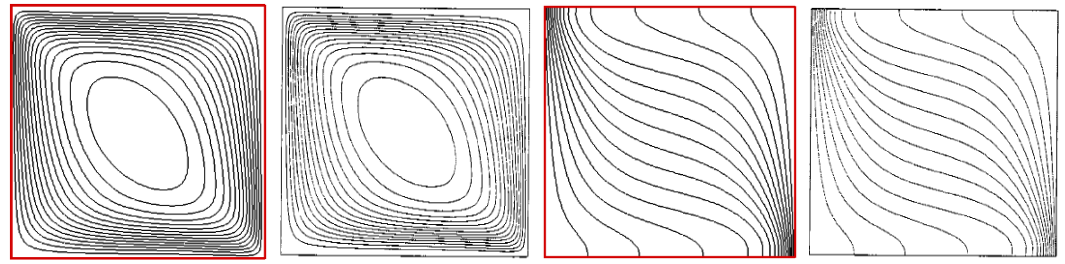

Streamline, Present work | Streamline, Sarris *et al*. (2006) | Isotherm, Present work | Isotherm, Sarris *et al*. (2006)

C

(c) Ra = 7×10^5, Ha = 100

Fig. 2. Validations; (a) - schematic of the computational domain with the specified boundary conditions for a buoyancy driven flow through square cavity under magnetic field, (b) - comparison of present code with the results obtained from Sarris (2006) *et al.* at Ra = 7×10^3 and Ha = 25 in cavity, (c) - comparison of present code with the results obtained from Sarris *et al.* (2006) at Ra = 7×10^5 and Ha = 100.

side walls, we used θ = 0 and 1, where $\theta = \frac{T - T_C}{T_H - T_C}$ in which the subscripts C and H refer to cold and hot walls, respectively. The comparison of streamline contours and isotherm lines obtained from the present code and those of Sarris *et al*. (2006) for natural convection through the enclosure under magnetic field (see Fig. 2-(a)) are depicted at Ra = 7×10^3 , Ha = 25 and Ra = 7×10^5 , Ha = 100 in Figs. 2(b) and 2(c). The present numerical results show excellent accuracy with the literature.

For validation of the present algorithm in the case of natural convection in porous media, comparison of average Nu are performed with those of Nithiarasu *et al*. (1997) with Darcy-Brinckman model. These computations are performed at Ra = 10^3, 10^4, 10^5 and 5×10^5 and at Da = 10^{-2} and Φ = 0.9. As it can be seen from Table 1, there is very good agreement between present results and data available in the literature. There are many porous enclosure problems with magnetic effect, but most of them are based on Darcy model; in our study, the simulation of porous media is based on Darcy-Brinckman model. We could find no paper about porous enclosure problems with magnetic effect which is based on Darcy-Brinckman law. So we validated our computation for two above cases. For comprise the results of computer code with the results of literature in porous enclosure problems with magnetic effect, we validated results of present code against results of Mahmud and Fraser (2004): Consider a square porous enclosure with differentially heated side walls. Darcy's law is assumed to hold and magnetic force is acting along the direction of the gravity. Figure 3 shows the comparison of our computation and Mahmud and Fraser (2004) in Ra* = 100 and Ha* = 0, 5 and 10.

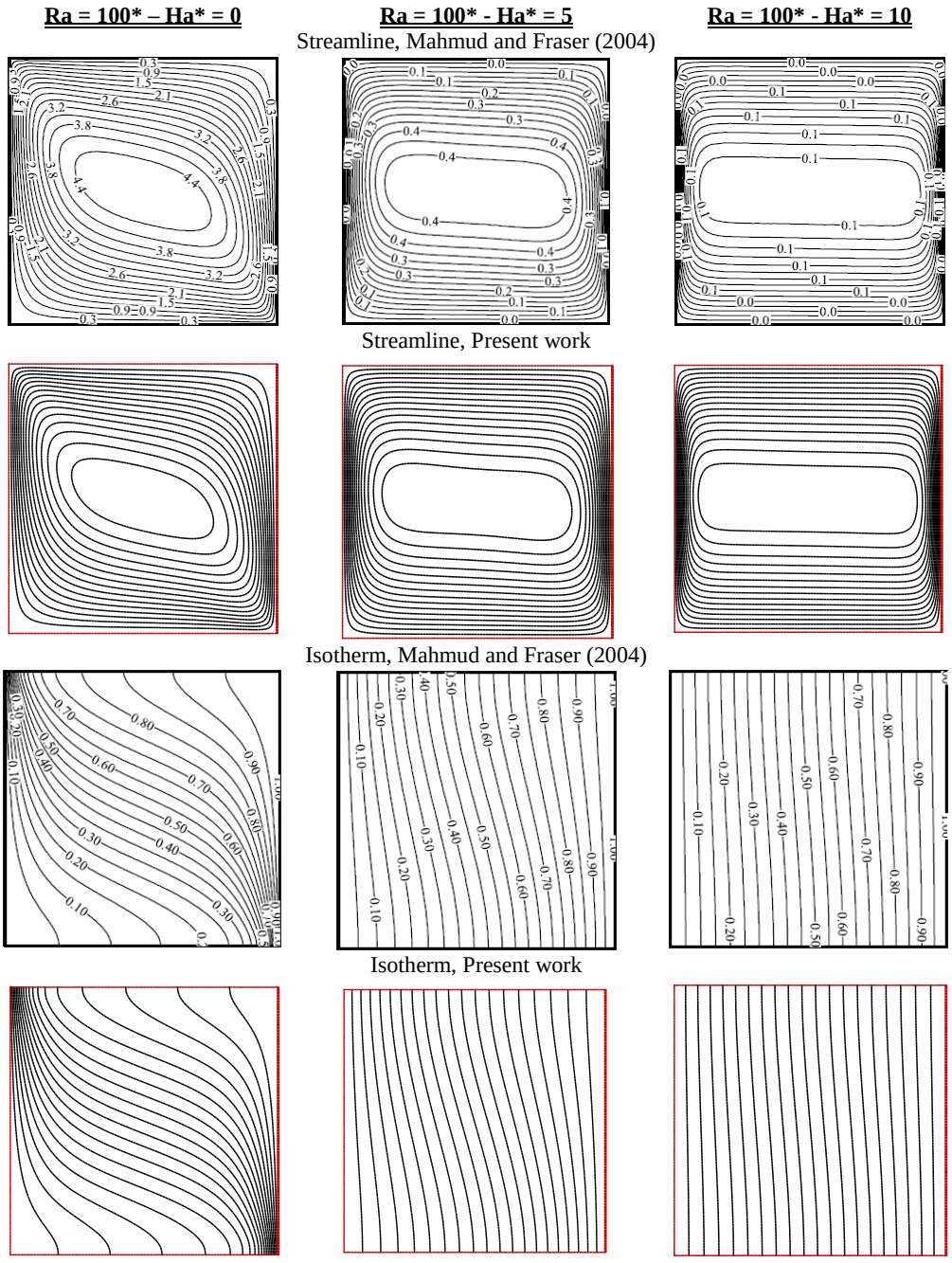

Fig. 3. Validations; comparison of present code with the results obtained from Mahmud and Fraser (2004) at Ra* = 100 and Ha* = 0, 5 and 10 in cavity.

Where Ra* is the product of Ra and Da and also Ha* is the product of Ha and Da. The comparison shows excellent accuracy of our computer code in which porous media comply from Darcy law.

Entropy generation is investigated for this problem and effect of different parameters on entropy generation is studied. In order to assess the accuracy of our numerical procedure for calculation of entropy generation, validation results can be seen in Fig.4.

Figure 1 shows the computational domain used in this study. As noted in this figure, the computational domain contains of porous inclined cavity with one/two rectangular partitions attached to adiabatic walls (see figure 1-(b)); where C_1 and C_2 are partition center distance from the hot wall. In this study C_1 and C_2 are considered 0.5H and 0.25H respectively. Also W and L are considered 0.2H and 0.3H respectively.

The present computations have been carried out within the range of Hartmann number Ha: $0 \leq Ha \leq 150$, inclination angle φ: $0 \leq \varphi \leq 135^{o}$, the partition height L: $0 \leq L \leq 0.4H$, and partition location are performed to individually investigate the influence of each of these parameters. Darcy number (Da) and porosity (Φ) of porous domain is considered 10^{-4} and 0.9, respectively. Prandtl number (Pr) is considered unity.

The irreversibility distribution ratio is taken equal to 10^{-3} in all calculations as given in Varol *et al.* (2008). Anyhow we have studied the effect of the irreversibility distribution ratio on overall entropy generation and Bejan number as shown in Fig. 5 for φ = 0.01, 0.001, 0.005 and 0.0001. As seen in this figure, as φ increases, overall entropy generation increases, but Bejan number decreases. As shown in this figure, at low and moderate Ra, with magnetic force, conduction dominates. Most of the contribution on overall entropy generation comes from the heat transfer irreversibility. So, Bejan number shows a value closer to 1 and the variation of OEG with increasing Ra is insignificant in low Ra. A significant contribution on OEG comes from the fluid friction irreversibility (FFI) at higher Ra due to high convection current.

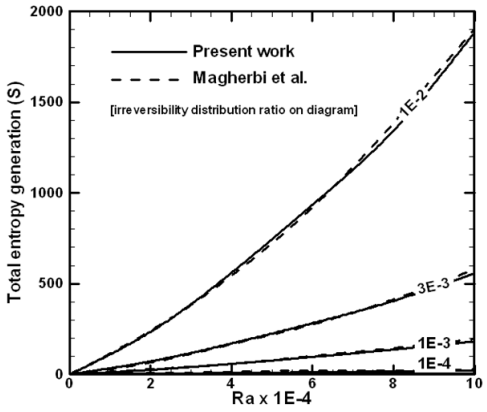

Fig. 4. Validation of entropy generation with Magherbi *et al.* (2003).

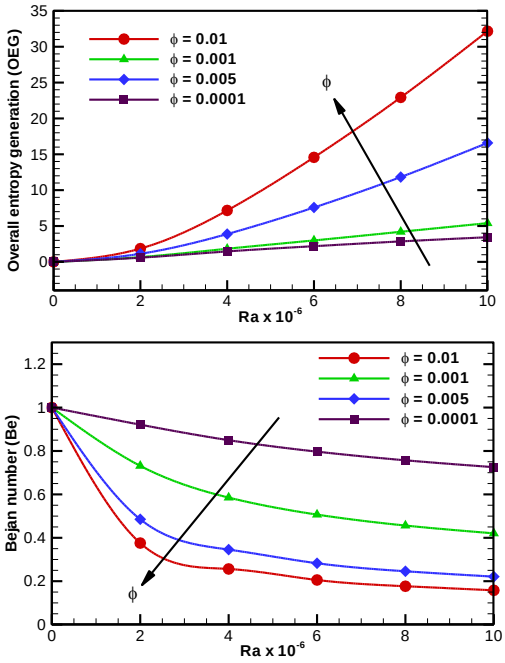

Fig. 5. The effect of irreversibility distribution ratio (ϕ) on overall entropy generation (OEG) and Bejan number (Be) at different Ra number with one partition.

Figure 6 depicts the variation of average Nusselt number versus height of partition L: $0 \le L \le 0.4H$ and at various Hartmann number: Ha = 0, 50, 100. In this case, one partition was attached to bottom wall of cavity (see Fig.1-(b)). It is observed that as L increases, the Nusselt number decreases which indicates that the convection heat transfer has been damped and this is due to the blockage effect. In each Ha, by locating of partition with L = 0.4H, average Nu can decrease by 20%.

Also from this figure, it was concluded that the magnetic field considerably decreases the average Nusselt number and as the Hartmann number increases, heat transfer from vertical walls decreases. So flow extremity due to thermo magnetic natural convection decreases. In Ha = 100, as partition height increases, average Nu can decrease by 25%.

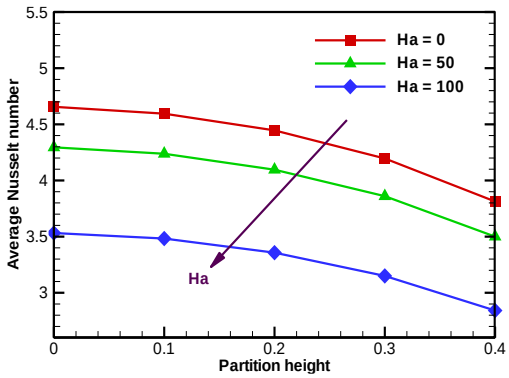

Fig. 6. Effect of partition height on average Nusselt number at various Ha in Ra = 5×10^6.

Figures 7-(a) and (b) show left wall average Nusselt number versus inclination angle in Ra = 5×10^6 for various Hartmann number: Ha = 0, 50, 100 and 150 with 1 and 2 partitions attached to horizontal wall (see Fig. 1-(b)).

These figures show that as the Hartmann number increases, heat transfer from vertical walls decreases. So flow extremity due to thermo magnetic natural convection decreases. That is, the application of a longitudinal magnetic field results in a force opposite to the flow direction that tends to drag the flow and as strength of the magnetic field is increased, convection is suppressed and the heat transfer in the enclosure decreases. As seen from these figures, with increase of inclination angle, Nu number firstly increases, but after 30º, it starts to decrease and also after φ = 105º Nu increases. In inclination angle about φ = 90º, average Nu for one and two partitions has different trends (see figures 7-(a) and (b)). In case of two partitions, Nu has lowest value. But in case of one partition, Nu is oscillated and afterwards that increases to φ = 135º. In this case, Nu in φ = 90º has local maximum. Also it's showed that in Various Ha, average Nu versus inclination angle has same trend (see figures 7-(a) and (b) again).

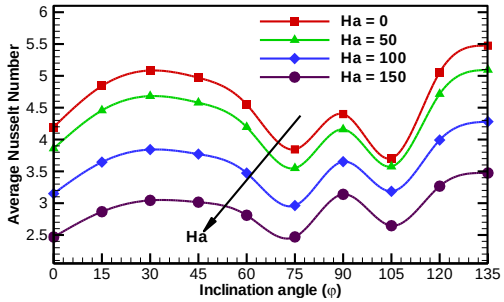

(a) One partition attached to horizontal wall

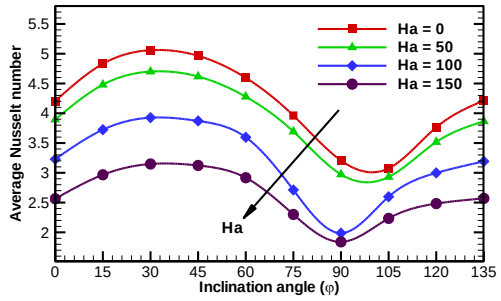

(b) Two partitions attached to bottom wall

Fig. 7. The average Nusselt number versus inclination angle in Ra = 5×10^6, (a) - one partition attached to bottom wall, (b) - two partitions attached to horizontal walls.

Figure 8 shows overall entropy generation, heat transfer entropy generation and Bejan number in various inclination angle for various Ha and Ra = 5×10^6 with 1 and 2 partitions attached to horizontal walls. As seen these figures, as Ha increases, because the convection term becomes less effective, so heat transfer entropy generation (HTI) decreases. Therefore overall entropy generation (OEG) decreases too. Increasing in the value of Ha has a tendency to slowdown the fluid movement inside the cavity, thus Bejan number enhances. These figures show that overall entropy generation and heat transfer entropy generation diagram has same trend with the average Nusselt number diagram except in φ = 90^o for one partition. In each inclination angle, as Nu increases, heat transfer entropy generation enhances and therefore overall entropy generation (OEG) increases. But Bejan number diagram has reverse trend with entropy generation diagram. As noted in Fig. 7, in inclination angle between 30^o and 45^o, OEG and HTI diagram has maximum value in case of one and two partitions. The minimum value of OEG and HTI diagram is in inclination angle about 105^o for one partition and about 90^o for two partitions. Also in inclination angle about 60^o, Bejan number diagram has minimum value in case of one and two partitions. The maximum value of Bejan number diagram is in inclination angle about 105^o for one partition, while it is about 90^o for the case of two partitions. In the other hand, in inclination angles which OEG and HTI diagram has lowest value, most of the contribution on overall entropy generation comes from the heat transfer irreversibility. So, Bejan number shows a higher value and in these angles, Be has maximum value. But in local maximum of OEG and HTI diagram, OEG and HTI curves have more difference, so the effect of fluid friction entropy generation increases and Be decreases.

Isotherms and streamlines contours for Ra = 5×10^6 with 1 and 2 partitions attached to horizontal walls depicted in Figs. 9 and 10 for Ha = 0 and 150. It is shown that as Ha increases the convection term becomes less effective. As shown these figures, in inclination angle equal to 90^o with 1 partition, two vertices are formed but with 2 partitions and also in other angles, one primary vortex is appeared in the enclosure. Also it is observed that in φ = 0^o, 45^o and 135^o in the middle of left wall and in the top of right wall thermal boundary layer is formed but in φ = 90^o for one partition, this boundary layer is diminished.

With comparing of figures 7 to 10 in φ = 90^o, it could be seen that with 1 partition the average Nusselt number diagram has local maximum, because in this case, the number of stream line loops in stream line contours changes to two loops and the average Nusselt number increases suddenly. But overall entropy generation in this case has low value and Bejan number in this angle has high value. So when we need local maximum in heat transfer, addition of the partition and rotating of cavity to 90^o would be best method.

REFERENCES

Abdul Hakeem, A. K., S. Saravanan and P. Kandaswamy (2008). Buoyancy convection in a square cavity with mutually orthogonal heat generating baffles. *International Journal of Heat and Fluid Flow* 29, 1164–1173.

Basak, T. and S. Roy (2005). Finite element analysis of natural convection flows in a square cavity with non-uniformly heated wall(s). *International Journal of Engineering Science* 43, 668-680.

Basak, T., S. Roy, T. Paul, and I. Pop (2006). Natural convection in a square cavity filled with a porous medium: Effects of various thermal boundary conditions. *International Journal of Heat and Mass Transfer* 49, 1430–1441.

Baytas, A. C. (2000). Entropy generation for natural convection in an inclined porous cavity. *International journal of Heat and Mass Transfer* 43, 2089–2099.

Bejan, A. (1994). *Entropy Generation Through Heat* and Fluid Flow, John Wiley & Sons 98-116.

Bilgen, E. and R. B. Yedder (2007) Natural convection in enclosure with heating and cooling by sinusoidal temperature profiles on one side. *International Journal of Heat and Mass Transfer* 50, 139–150.

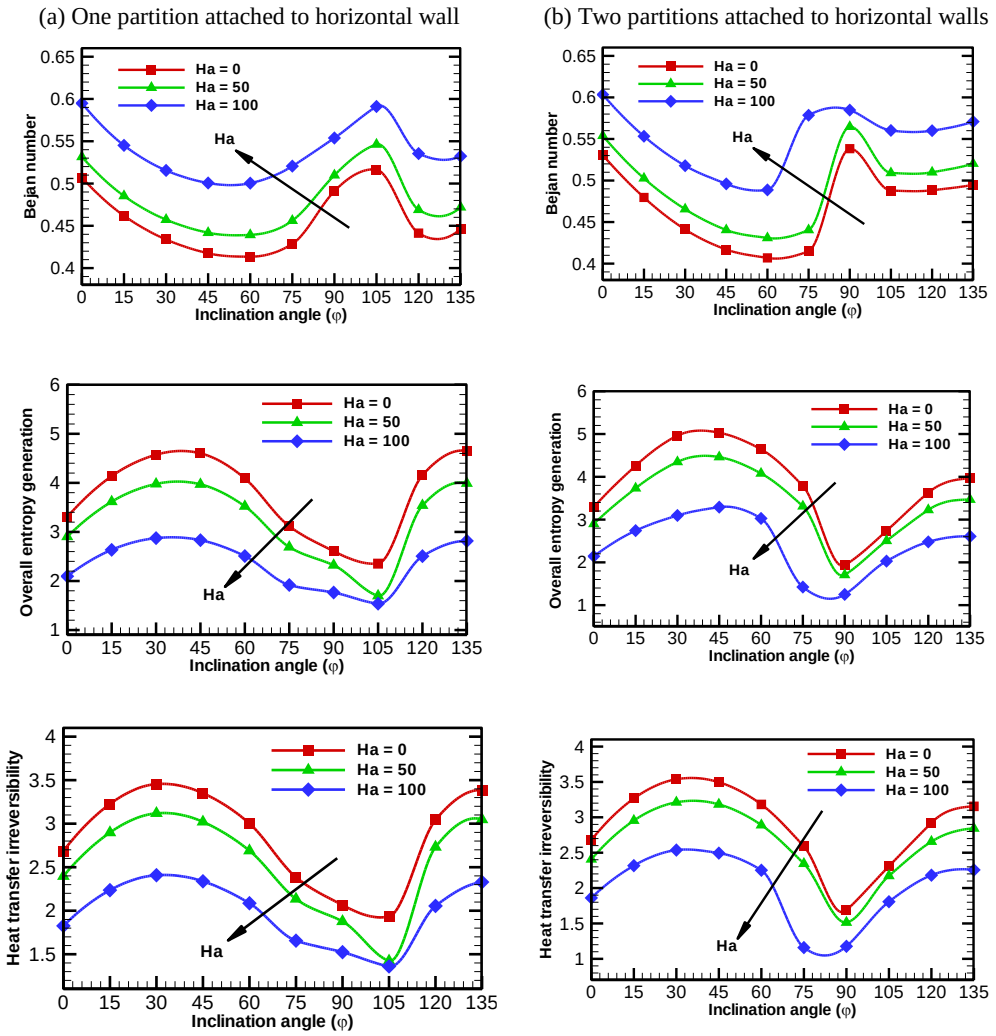

Fig. 8. The effect of inclination angle on overall entropy generation (OEG), heat transfer irreversibility (HTI) and Bejan number (Be), Ra =5×10^6, (a) - one partition attached to bottom wall, (b) - two partitions attached to horizontal walls.

Ece, M. C. and E. Büyük (2006). Natural convection flow under a magnetic field in an inclined rectangular enclosure heated and cooled on adjacent walls. *Fluid Dynamics Researc* 38, 564–590.

Famouri, M. and K. Hooman, (2008). Entropy generation for natural convection by heated partitions in a cavity. *International Communications in Heat and Mass Transfe* 35, 492-502.

Grosan, T., C. Revnic, I. Pop and D. B. Ingham (2009). Magnetic field and internal heat generation effects on the free convection in a rectangular cavity filled with a porous medium. *International Journal of Heat and Mass Transfer* 52, 1525–1533.

Heidary, H., M. Davoodi and M. J. Kermani (2009). Numerical solution of free convection in a rectangular cavity filled with a porous medium and non uniform boundary condition, *Proc. 4th International Conference on Application of Porous Media*, Istanbul, Turkey.

Jue, T. (2006). Analysis of combined thermal and magnetic convection ferrofluid flow in a cavity. *International Communications in Heat and Mass Transfer* 33, 846–852.

Kaluri, R. S., and T. Basak (2011). Role of entropy generation on thermal management during natural convection in porous square cavities with distributed heat sources. *Chemical Engineering Science* 66, 2124-2140.

Kaluri, R. S. and T. Basak (2011). Analysis of entropy generation for distributed heating in processing of materials by thermal convection. *International Journal of Heat and Mass Transfer* 54, 2578-2594.

Kandaswamy, P., J. Lee, A. K. Abdul Hakeem and S. Saravanan (2008). Effect of baffle–cavity ratios on buoyancy convection in a cavity with mutually orthogonal heated baffles. *International Journal of Heat and Mass Transfer* 51, 1830–1837.

Ha = 150 Ha = 0

(a) Streamline Contours, One partition attached to bottom wall

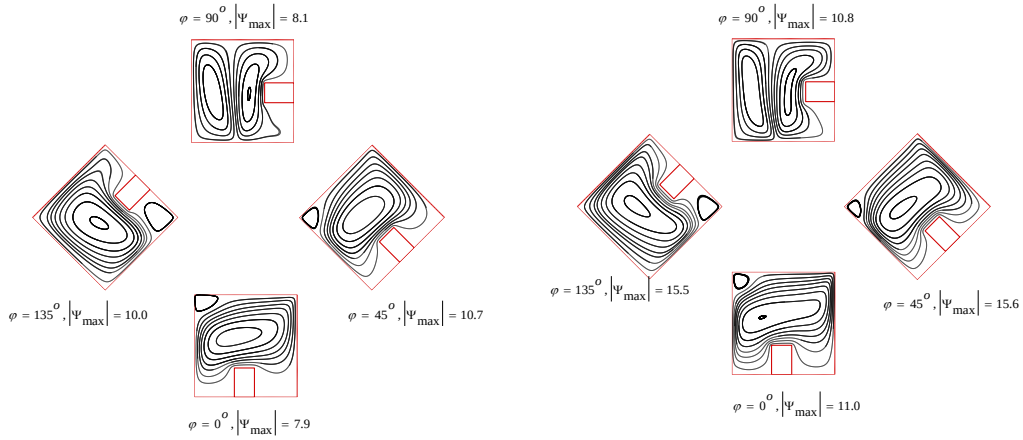

(b) Streamline Contours, Two partitions attached to horizontal walls

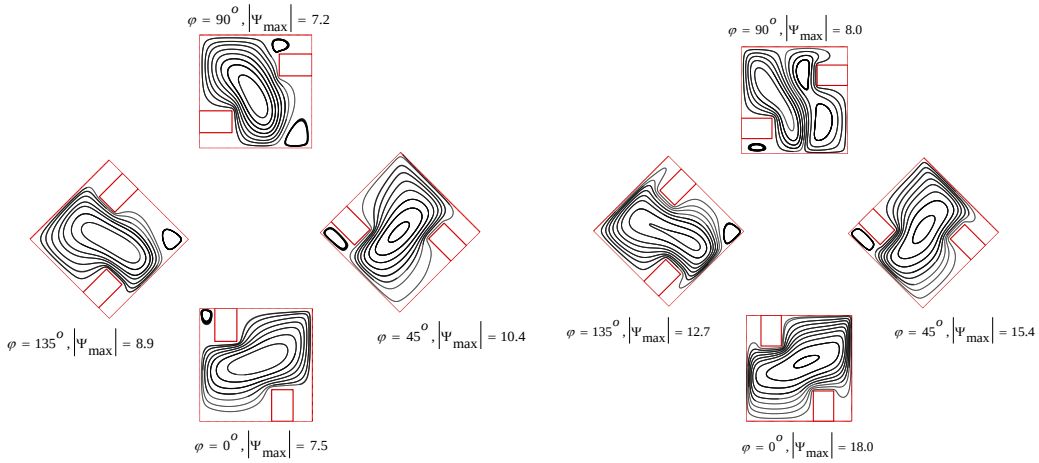

Fig. 9. Streamlines contours for φ = 0⁰, 45⁰, 90⁰ and 135⁰ in counterclockwise direction for Ra = 5×10⁶ for Ha = 0 and 150; (a) - one partition attached to bottom wall, (b) - two partitions attached to horizontal walls.

Khanafer, K., N. M. Al-Najem and M. M. El-Refaee (2000). Natural Convection in Tilted Porous Enclosures in the Presence of a Transverse Magnetic Field. *Journal of porous media* 3, 79-91.

Krakov, M., and I. V. Nikiforov (2005). Thermo magnetic convection in a porous enclosure in the presence of outer uniform magnetic field. *Journal of Magnetism and Magnetic Materials* 289, 278–280.

Magherbi, M., H. Abbasi and A. Ben-Brahim (2003). Entropy generation at the onset of natural convection. *International Journal of Heat and Mass Transfer* 46, 3441–3450.

Magherbi, M., A. El Jery, N. Hidouri and A. Ben Brahim (2010). Evanescent magnetic field effects on entropy generation at the onset of natural convection. *Sadhana - Academy Proceedings in Engineering Sciences* 35, 163-176.

Mahmud, S. and R. A. Fraser (2004). Magneto-hydrodynamic free convection and entropy generation in a square porous cavity. *International Journal of Heat and Mass Transfer* 47, 3245-3256.

Mahmud, S., R. A. Fraser and I. Pop (2007). Flow, thermal, energy transfer, and entropy generation characteristics inside wavy enclosures filled with microstructures. *Journal of Heat Transfer* 129, 1564-1575.

Merrikh, A. A. and A. Mohamad (2000). Transient Natural Convection in Differentially Heated Porous Enclosures. *Journal of porous media* 3.

Narusawa, U. (2001). The second-law analysis of mixed convection in rectangular ducts. *Heat*

Ha = 150 Ha = 0

(a) Isotherm Contours, One partition attached to bottom wall

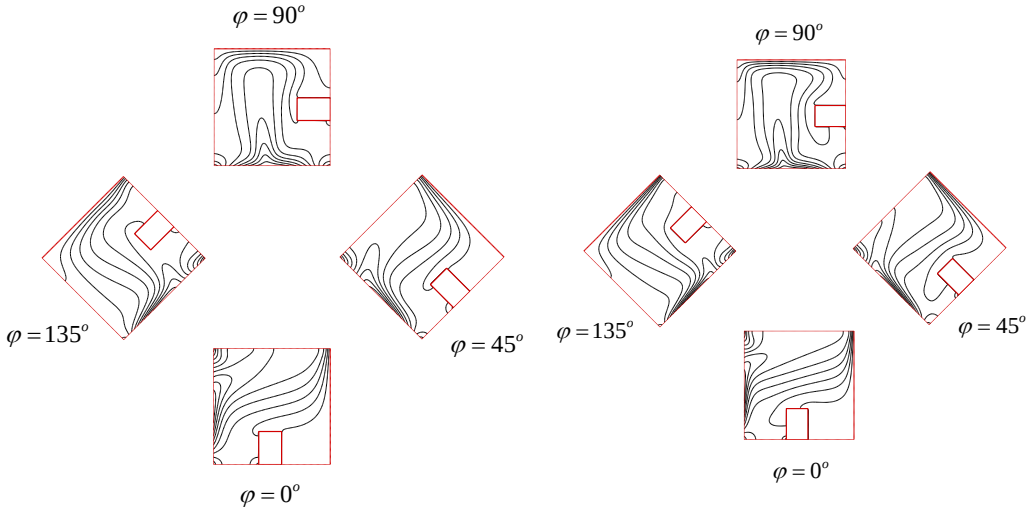

(b) Isotherm Contours, Two partitions attached to horizontal walls

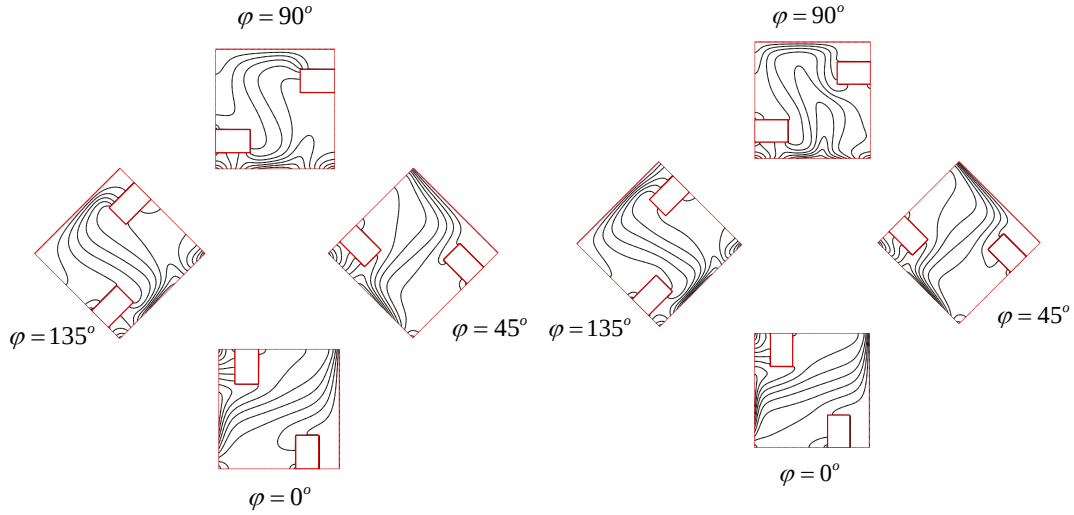

Fig. 10. Isotherm contours for φ = 0^0, 45^0, 90^0 and 135^0 in counterclockwise direction for Ra = 5×10^6 for Ha = 0 and 150; (a) - one partition attached to bottom wall, (b) - two partitions attached to horizontal walls.

and Mass Transfer 37, 197–203.

Nield, D. A. (1999). Modeling the effects of a magnetic field or rotation on flow in a porous medium: momentum equation and anisotropic permeability analogy. *International Journal of Heat and Mass Transfer* 42, 3715-3718.

Nithiarasu, P., K. N. Seetharamu and T. Sundararaja (1997). Natural convective heat transfer in a fluid saturated variable porosity medium. *International Journal of Heat and Mass Transfer* 40, 3955–3967.

Patankar, S. V. and D. B. Spalding, (1972). A calculation procedure for heat, mass and momentum transfer in three-dimensional parabolic flows. *International Journal of Heat and Mass Transfer* 15, 1787–1806.

Pirmohammadi, M. and M. Ghassemi (2009). Effect of magnetic field on convection heat transfer inside a tilted square enclosure. *International Communications in Heat and Mass Transfer* 36, 776-780.

Rhie, C. M. and W. L. Chow (1983). Numerical study of the turbulent flow past an airfoil with trailing edge separation. *AIAA journal* 21, 1525–1532.

Rosen, M. A. (1999). Second-law analysis: approaches and implications. *International Journal of Energy Research* 23, 415–429.

Saeid, N. H. (2005). Natural convection in porous

cavity with sinusoidal bottom wall temperature variation, *International Communications in Heat and Mass Transfer* 32, 454–463.

Sarris, I. E., G. K. Zikos, A. P. Grecos and N. S. Vlachos (2006). On the limits of validity of the low magnetic Reynolds number approximation in MHD natural-convection heat transfer. *Numerical Heat Transfer* 50, 158–180.

Storesletten, L. and I. Pop(1996)., Free convection in a vertical porous layer with walls at non-uniform temperature. *Fluid Dynamic Research* 17, 107–119.

Varol, Y., H. F. Oztop and A. Koca (2008). Entropy generation due to conjugate natural convection in enclosures bounded by vertical solid walls with different thicknesses. *International Communications in Heat and Mass Transfer* 35, 648–656.

Varol, Y., H. F. Oztop and A. Varol (2007). Natural convection in porous triangular enclosures with a solid adiabatic fin attached to the horizontal wall. *International Communications in Heat and Mass Transfer* 34, 19–27.

Zahmatkesh, I. (2008). On the importance of thermal boundary conditions in heat transfer and entropy generation for natural convection inside a porous enclosure. *International Journal of Thermal Sciences* 47, 339-346.